



---

# Bending stiffness and strength performance of different column splice connections

*F. Tork-Ladani, J.G. Chase & G.A. Macrae*

University of Canterbury, New Zealand.

## ABSTRACT

Tall steel structures are increasingly common in seismic zones, but their column design relies on splice connections to create tall structures. Bolted splice connections may exhibit greater flexibility during strong earthquake shaking than expected by design. Although the strength characteristics of these connections are defined in guidelines and (some) standards (NZS3404), their stiffness and ductility characteristics are less known. In particular, the moment-rotation performance of column splices significantly affects the seismic response and possibility of an undesirable local or global failure.

A series of moment tests were conducted on bolted and welded, bearing column splices across standard, universal column sections (310UC158, 310UC118) tested to failure. In particular, 3 bolted lap splice connections, 1 bolted end plate connection, and 1 welded splice connection. Specimens were quasi-statically tested in a Dartec machine. Flexural performance was assessed using moment-rotation hysteresis loop measurements at the splice to assess strength, stiffness and ductility.

The welded splice was the most rigid and strongest, exceeding guidelines. The end plate splice was stronger than existing guidelines expect, and less ductile than the lap splices, which were the most ductile. Lap splice strength also exceeded guideline expectations. Splice connections consistently exceed guideline expected strength and have widely varying stiffness.

## 1 INTRODUCTION

Since the moment-rotation performance of column splices affects both the structural dynamic response and possibility of an undesirable local or global failure, it is desirable if the performance can be quantified under the type of flexural loading demands such a splice may experience during earthquake shaking.

Column splices are required to develop certain amount of axial, shear and moment capacity as part of a gravity or moment frame. But the values differ in different standards. In US standards, the steel seismic design provisions, (AISC 341-10) clauses E2.6g and E3-6g, stipulate design flexural capacity of column splices in special and intermediate frames to be at least equal to the flexural strength of the smaller column. The shear strength of the splice is prescribed to satisfy the demand associated with the flexural hinging at both ends of the column assuming double curvature deflection. Current (NZS 3404) design specifications for column splices, in frames required to resist significant seismic forces (i.e. Category 1 and 2 frames), require the connection to provide 50% of the reduced flexural design strength of the smaller column (i.e.  $\phi M_r$ ), as well as 25% of its design shear capacity.

Welding and bolting are two common methods of fabricating splices. While welded splices act as rigid connections, rotation is very likely to occur in bolted splices. Currently, there is not any specific provision for the required stiffness of splices for an earthquake event, which may affect overall frame performance. If splices are strong enough to carry the demand, but not sufficiently stiff, they may exhibit large deformations at a certain level of strength, which could be detrimental.

There are few experimental research studies addressing shear and flexural performance of column splices. (Bruneau et al.) performed moment tests on partial and full penetration butt welded splices in heavy steel sections subjected to pure bending. (Stillmaker et al.) conducted analytical and experimental studies on partially welded column splices and proposed a method for seismic design of partially welded column splices.

(Edwards et al.) performed monotonic pure moment experiments on major and minor axis behavior of welded-bolted splices in H-section columns. The connections tested are not a common way of splicing in modern practice. (Douty et al.) studied the performance of beam splices under monotonic pure moment loading as part of beam-column connection investigations. (Beedle et al.) reported two moment experiments conducted at University of Cambridge in 1958 on beam splices. One of the specimens was designed as a riveted full plastic moment splice, where rivets were substituted with bolts. The other was connected by half as many bolts.

The literature mainly provides an overview of strength of these connections under monotonic loading, but does not investigate the stiffness behavior. There is a need to understand column splice strength and stiffness behaviour so that the implications of different characteristics on the dynamic response of realistic building systems may be developed, so that design approaches may be checked or developed to prevent undesirable building response. This paper summarizes the results of several experiments on different column splice connections to address:

- The flexural strength of splices designed for various levels of design actions about the major axis
- The effect of web cover plate in carrying major axis moment
- The stiffness performance of different methods of column splice construction
- The implication of the experimental findings for construction practice

## 2 METHODOLOGY

### 2.1 Test Setup

Figure 1 shows the moment test setup using the Dartec 10MN universal testing machine. Four columns, not shown in the figure, support the rigid roof of the Dartec, which can be adjusted at any height. A hydraulic actuator at the bottom of the machine applies vertical forces.

The top and bottom setup beams are attached to the Dartec by four 51mm bolts of high strength steel, AISI 4140. While the bottom beam can move up and down with the actuator, the top beam is fixed to the Dartec

roof and is stationary. Special connections were designed to facilitate the cyclic loading. The connections accommodate two rollers each side of the specimens at the loading and supporting points. The rollers are pinned to two plates with slotted holes. This design restrains the ends of the rollers from vertical movements, while providing freedom for the test specimen to move horizontally.

Three M36 Grade 10.9 threaded rods are located at each side of the specimen to clip the rollers to the specimen. The threaded rods are tightened sufficiently to keep the rollers on the specimen, avoiding pre-tensioning of threaded rods and restraining horizontal movement of the specimen. The connections are fixed to the top and bottom beams with rigid pedestals. Eight M24 high strength bolts connect the blocks to the setup beams.

When the actuator moves up, the end bottom rollers push up the specimen ends and the middle top rollers, apply downwards force on the specimen. When the actuator moves down, the forces are applied in the opposite direction through the opposite rollers. In this state, the threaded rods are engaged to transfer the forces. This setup provides constant moment between the loading points without a significant shear force. Although the right end rollers were restrained from rolling, it was observed the specimen could slip under heavy loads. Therefore, a link was provisioned to stop the slippage while allowing the end to rotate.

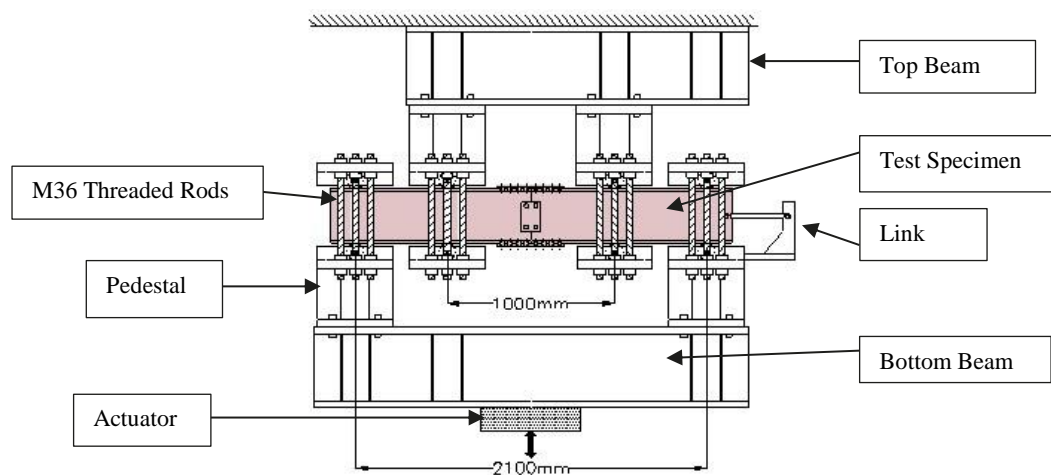


Figure 1: Test setup components

## 2.2 Loading Regime

The loading in this study was controlled by the displacement of the actuator. This displacement is different from the displacement at the centre of the specimens. Since the bolts attaching the setup to the Dartec could not be post-tensioned due to the large diameter, the joints experienced some slack when the actuator is in tension. Therefore, the specimens themselves were subjected to smaller displacements in the direction corresponding to actuator tension. The loading regime slowly applied to the actuator in the experiments is shown in Figure 2. The range of motions was chosen to ensure yielding and failure in a well-incremented set of steps. No axial load was applied to the specimens during the moment tests.

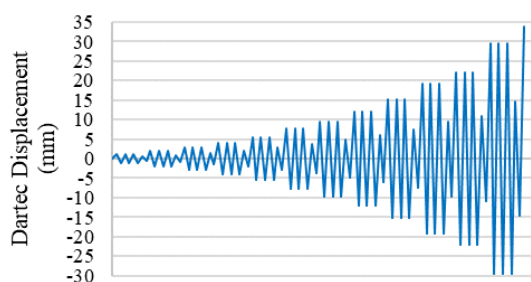


Figure 2: Loading regime applied to Dartec actuator

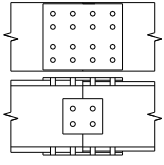
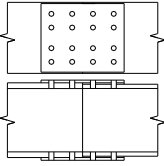
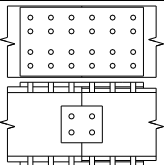
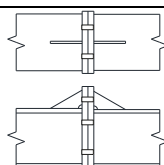
## 2.3 Test Specimens

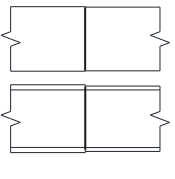
Bolted splice connections are commonly used in New Zealand practice due to faster construction on site. An equivalent welded specimen was also tested in bending to compare the behaviour of the connections. Universal Column sections were used for all experiments. Bolted splices were fabricated with end plates and lap-splice plates. The splice specimens were made of 310UC158 and 310UC118 column sections, Grade 300. The pair provides complete bearing area at the contact surface of the sections. All connections were designed in alignment with current standards/practice.

Specimen #1 targeted the minimum design bending and shear actions prescribed in the New Zealand Steel Structures Standard, NZS3404 clause 12.9.2.2, for seismic columns in ductile moment frames. These specifications are 50% of the reduced moment capacity of the smaller section at the splice joint ( $0.5\phi M_r$ ) and 25% of the reduced shear capacity ( $0.25\phi V_v$ ). Specimen #2 had the same flange splice components, but was not spliced at the web. Specimen #3 splice was stronger and targeted  $0.7\phi M_r$  of the smaller section capacity and 25% of the reduced shear capacity. Since the holes reduce the area of the section, the nominal section capacity decreases at the splice location to about  $0.75\phi M_p$  for all specimens.

Specimens #4 is an end plate bolted connection designed for approximately 50% of the reduced moment capacity. Specimen #5 is a fully butt welded joint to develop the full moment capacity of the smaller member. The details of the specimens are listed in Table 1.

Table 1: Lists of details of specimens

Specimen	Top and side views	Flange cover plate		Web cover plate		Flange bolts			Web bolts		
		Thickness (mm)	Grade	Thickness (mm)	Grade	Size	Number	Grade	Size	Number	Grade
#1		12	300	6	350	20	32	8.8	20	4	8.8
#2		12	300	-	-	20	32	8.8	20	-	-
#3		20	300	6	350	20	48	8.8	20	4	8.8
#4		32	350	-	-	24	8	8.8	-	-	-

#5		-	-	-	-	-	-	-	-	-
----	---	---	---	---	---	---	---	---	---	---

## 2.4 Design Principles

Specimens #1 to #3 were designed based on the model proposed in the Connection Design Guide 13, which is in accordance with Australian Standard AS 4100. The model assumes moment demand is transferred through the flange splice plates acting in tension and compression, while the web splice plates transfer shear demand. No interaction between the web and flange splices is considered (Connection Design Guide 13).

Splice connections with Category 8.8/TF bolts are used to limit slip at service level loads. For the flange splice configuration of Specimens #1 and #2, slip is estimated to occur at  $0.24M_p$  assuming the friction coefficient is 0.35 for rolled steel surfaces (NZS3404), and tension per M20 bolt at installation (proof load) is 145kN without considering the capacity reduction factor, 0.7, at serviceability limit state. Slip is predicted at  $0.36M_p$  for the flange splice configuration of Specimen #3, based on (Connection Design Guide 13).

For Specimen #4, the end plate splice, was designed in accordance with (HERA REPORT R4-100.1:2003). To develop sufficient rigidity in the connections with plates thinner than 20mm, the model requires the plate and bolt strength not to be governed by formation of four plastic hinges in an equivalent T stub. In this case, the top or the bottom bolt group/plate tension capacity limits the moment capacity of the connection, while the other bolt group is assumed to transfer shear actions.

No specific design was required for Specimen #5. The abutted joint was welded through the full thickness of web and flanges by a qualified welder. The estimated capacity for each component of the specimens are listed in Tables 2. All estimations are based on the reduced design capacities of the components.

Table 2: Design details of specimens

Specimen	Design capacity of flange splice				Design capacity of web splice			
	Plate component		Bolt component		Plate component		Bolt component	
	Capacity	Failure mode	Capacity	Failure mode	Capacity	Failure mode	Capacity	Failure mode
#1	$0.5\phi M_p$	Plasticity in the net area	$0.44\phi M_p$	Shear in bolt	$0.58\phi V_y$	Shear failure	$0.34\phi V_y$	Interaction of shear and induced moment
#2	$0.5\phi M_p$	Plasticity in the net area	$0.44\phi M_p$	Shear in bolt	-	-	-	-
#3	$0.84\phi M_p$	Plasticity in the net area	$0.67\phi M_p$	Shear in bolt	$0.58\phi V_y$	Shear failure	$0.34\phi V_y$	Interaction of shear and induced moment
#4	$0.64\phi M_p$	Two plastic hinges in T-stub	$0.46\phi M_p$	Tension in bolt	$5.3\phi V_y$	Transverse tearing in bolt hole 1 <sup>st</sup>	$0.99\phi V_y$	Shear in bolt
#5	Full penetration butt weld				Full penetration butt weld			

## 2.5 Fabrication of Test Specimens

Specimens were constructed using 310UC158 and 310UC118 columns. The dimensional difference of the sections is 12mm, which is filled by two 6mm-filler plates on each side. Two web splice plates of thickness of 6mm were used on both sides of the webs. Since the difference in the web thicknesses was less than 3mm on each side, no filler was used to fill the gap. The plates bent slightly when the web bolts were tightened.

High strength zinc-plated bolts, fully threaded through the length, were used to connect the flange splice plates. Web bolts were from the same material, but partially threaded. Standard flat round washers for high strength structural M20 bolts are 3.1-4.6mm thick and their outside diameter is 37-39mm. The washers supplied with the bolts were later found to be approximately 1-2mm thick and 37mm of outside diameter. The holes were drilled using drill bits. All the holes were 2mm oversized,

In Specimen #1, the contact surfaces were contaminated with some drilling oil and loose particles before assembling the parts. For the rest of the specimens the contact surfaces were cleaned with a wire brush to remove the loose mill scale and then wiped with solvent to remove any contamination with drilling oil.

The bolts in Specimen #1 were tightened with a torque wrench set to apply 145N.m. However, the recommended torque by the fabrication company to get to about 65% of the proof load is 372N.m. For the rest of similar specimens, the bolts were proof tightened with 1/3 of a full turn as recommended by the manufacturer to obtain 145kN tension in the bolts. This value was more tightening than that for bolts in Specimen #1.

Specimen #4 is an end-plate bolted splice. The M24 bolts are partially threaded with 40mm unthreaded length. The end-plates experienced distortion due to welding. This distortion caused a gap of 0-1.5mm between the plates. The bolts were proof tightened with 1/3 of a full turn as recommended by the manufacturer to obtain 210kN tension in bolts.

## 2.6 Instrumentation and Interpreting Readings

Two linear potentiometers were attached horizontally to the top and bottom flanges to measure the gap between the spliced members as shown in Figure 3. The data provides the rotation at the splice joint at each load step. Other instrumentation devices seen in the photo are not the subject of this study.

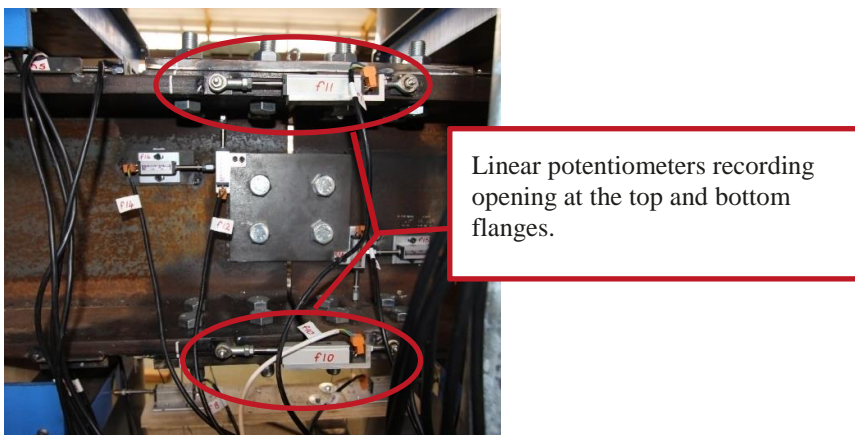


*Figure 3: Linear potentiometer measuring gap between the two sections*

Figure 4 shows the bending moment diagram resulting from the applied loads. The moment and rotation at the connection were calculated as shown in Figure 5. These calculations translate measurements into resulting loads and actions.

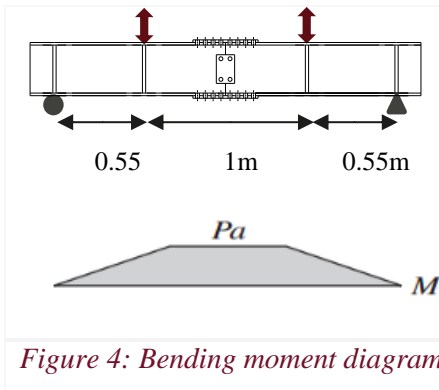


Figure 4: Bending moment diagram

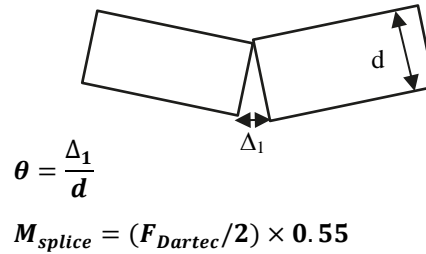


Figure 5: Force deformation relationships

### 3 RESULTS AND DISCUSSION

#### Specimen #1

The hysteresis behaviour of the connection is shown in Figure 6. The connection developed ~76% of the nominal plastic moment capacity of the smaller section associated with ~8% rotation at the joint.

The expected slip at the connection mainly occurs on the tension side. If the bolts are centered in the 2mm oversized holes, the rotation anticipated before bolt bearing occurs is approximately  $4\text{mm}/327\text{mm} = 0.012$  or 1.2%, as there are two holes either side of the splice and 2mm oversized yielding 4mm motion. Figure 6 shows the actual rotation before load increased significantly was about 2%. After dismantling the specimen, the bolt threads were observed to have penetrated into the plates, as seen in Figure 7. The minor diameter of M20 bolts is approximately 3mm smaller than the nominal diameter. Therefore, the threads are 1.5mm high, and the rotation anticipated after bolt bearing occurs is approximately  $7\text{mm}/327\text{mm} = 0.021$  or 2.1%, which better matches the 2% value seen in the hysteresis loop of Figure 6.

The bolts were snug-tightened with a hand torque wrench set to apply 145N.m. This value was less than the torque recommended by the fabrication company to obtain approximately 65% of the proof load, which was 372Nm. The likely axial force was thus about  $65\% \times (145\text{kNm}/372\text{kNm}) \times \text{PROOF LOAD (145 kN)} \times \text{N bolts} = 65\% \times 145\text{kNm}/372\text{kNm} \times 145\text{kN} \times 8 \text{ bolts} = 294\text{kN}$ .

The loops corresponding to the second and third cycles after the slippage show slackness and gapping due to hole elongation. The maximum elongation in the splice plates and the shear deformation in the bolts were approximately 4mm and 5mm, respectively. These values allows a  $2 \times 9\text{mm}/327\text{mm} = 0.055$  rotation after slippage. This latter result is consistent with the post-slippage displacement of about 6% seen in Figure 6.

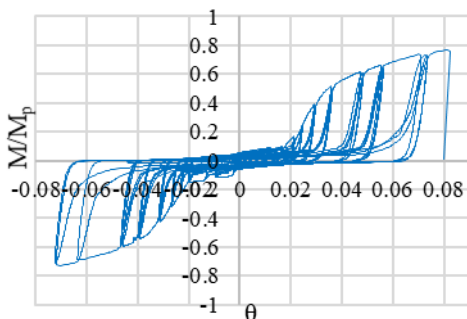


Figure 6: Hysteresis loop: moment ratio ( $M/M_p$ ) vs rotation  $\theta$

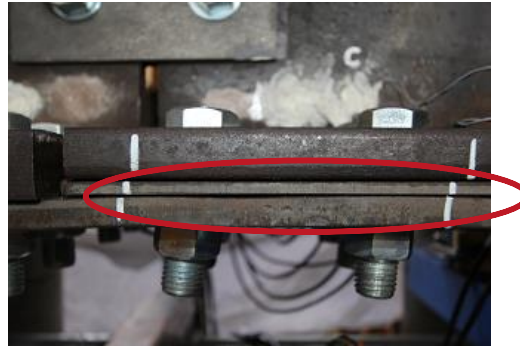
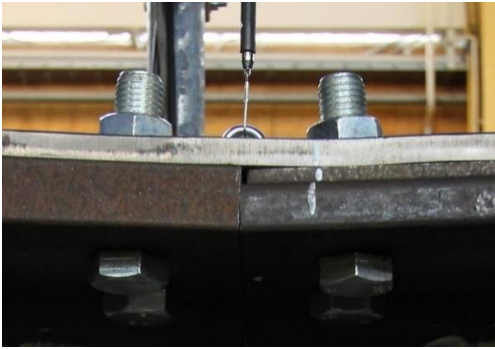


Figure 7: Threads in holes due to bearing of bolts

The bolts on the bottom splice plate of the smaller member failed in shear and the bolts were projected out with a very high speed similar to an explosion. While the bending/prying of the splice plates on the

compression side puts tension on the bolts, this tension did not seem to adversely affect the splice flexural strength. Figure 8 illustrates bending of splice plates on the compression side.

Figure 9 shows the separation of the splice plate and the filler plate close to connection's failure. The damage could be attributed to prying actions and piled up material at the bearing area of the bolts. Figure 10 shows damage in the flange splice plate. It is seen that all the holes yielded in bearing and the plate yielded along the inner row of the bolt holes. The resulting deformation allowed the inner bolts to tilt more. It is also clear that the hole ovalization is larger for the inner rows compared to the edge rows. Figure 11 shows the damage in the web holes. Although it is assumed web splices do not participate in transferring bending moment, they could damage in large rotations, which could potentially affect their shear performance.



*Figure 8: Bending in splice plate on compression side*      *Figure 9: Gap between connection plates*



*Figure 10: Damage in flange splice plate*      *Figure 11: Elongation of holes in web*

## **Specimen #2**

This test was conducted to study the effect of eliminating the web splices in Specimen #1 on flexural performance of the connection. Figure 12 shows the hysteresis behaviour of the connection. The ultimate strength is approximately  $0.73M_p$ , which is slightly less than that of Specimen #1. The small variation could be because of the small lever arm for the web splice bolts, small ratio of the number of bolts in the web to flanges and thin web and web splice plates in Specimen #1, which led to elongation of the holes. Specimen #2 is also more flexible at larger rotations than Specimen #1, which is likely to be as a result of the absence of web splice.

The bolts in Specimen #2 were tightened to obtain 145kN tension. Initially, the friction force in this case is about  $0.2M_p$ , which is very close to the estimated value.

The slip force is greater than that of Specimen #1 due to different surface preparations and higher tension in the bolts. However, the slip force dropped to less than  $0.1M_p$  in the larger displacement cycles. The connection rotational capacity is 0.084, which is 5% more than that of Specimen #1.

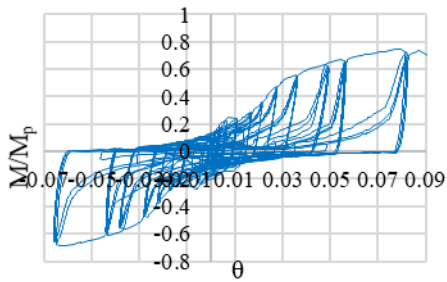


Figure 12: Hysteresis loop: moment ratio ( $M/M_p$ ) vs rotation  $\theta$

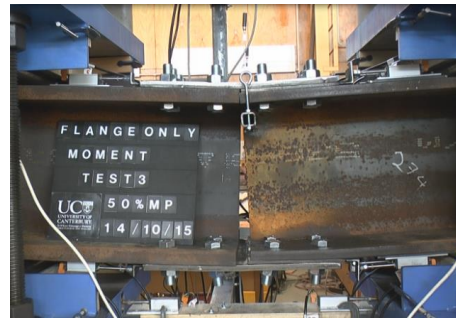


Figure 13: Deformation in Specimen #2 close to failure

The failure mode was similar to that of Specimen #1. Figure 14 shows abrasion and splitting of the hole edge, which was also observed in Specimen #1. Figure 15 shows the gap at the spliced joint during the experiment at zero load as observed in Specimen #1. Figure 16 shows deformation in one of the bolts at failure. It can be seen the upper portion of the bolt has tilted. Similar deformation of bolts were observed in Specimen #1.



Figure 14: Abrasion and splitting of hole edges in filler plates



Figure 15: Elongation at splice joint



Figure 16: Deformation of bolt at failure

### Specimen #3

Specimen #3 was designed for higher strength than Specimen #1, to compare the overall performance of splices designed for different strengths. Figure 17 shows the hysteresis behaviour of the connection. The connection ultimate strength capacity is greater than  $M_p$  even though holes were present in the flanges. This overstrength could be attributed to strain hardening in the flanges and the contribution of the splice plates. The connection exhibits larger stiffness compared to Specimen #1. Initially, the friction force in this case is about  $0.22-0.28M_p$ , which is smaller than the estimated value.

The connection has smaller rotational capacity compared to the other two specimens possibly because the thicker (20mm) flange splice plate was stronger and had less bolt hole deformation under the forces imposed by the bolts. In addition, the bending stiffness of the flange plates are larger than for Specimen #1.

Figures 19 and 20 show damage in the smaller member. The column flanges and web are damaged more than in Specimen #1. The smaller member yielded adjacent to the splice joint. This behaviour could indicate that the splice joint was not the weakest bending point in the member. No significant elongation was observed at the holes in the flange splice plate. The failure mode was similar to that of Specimen #1.

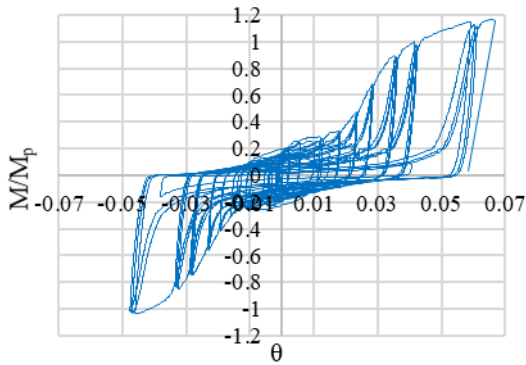


Figure 17: Hysteresis loop: moment ratio ( $M/M_p$ ) vs rotation  $\theta$

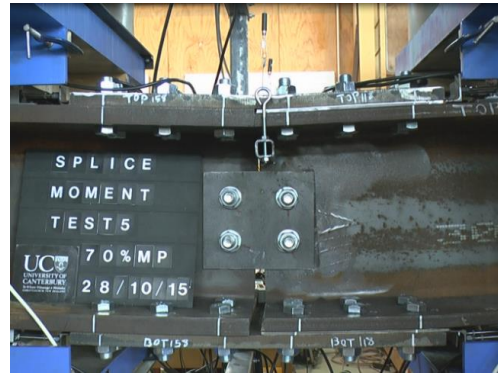


Figure 18: Deformation in Specimen #3 close to failure



Figure 19: Damage in flange in smaller member

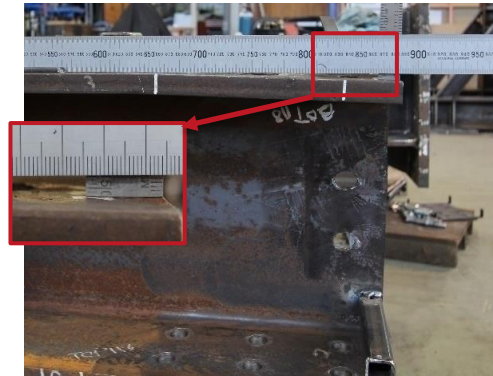


Figure 20: Damage in flange and web in smaller member

#### Specimen #4

This test was conducted to study the difference in the flexural performance of lap bolted splice connections relative to end plate splice connections. The cyclic performance of the connection is shown in Figure 21. The rotational capacity of the specimen is considerably smaller than the lap splice connections. The elastic deformation is approximately 0.001 or 0.1%, which could be due to elastic elongation of bolts.

The ultimate deformation of the connection is approximately 1.56%, which is associated with approximately 6mm elongation in the farthest bolts assuming zero deformation in the end plates. The ultimate strength is approximately  $0.78M_p$  compared to the  $0.46\phi M_p$  calculated in Table 2. As expected, the failure occurred in the bolts.

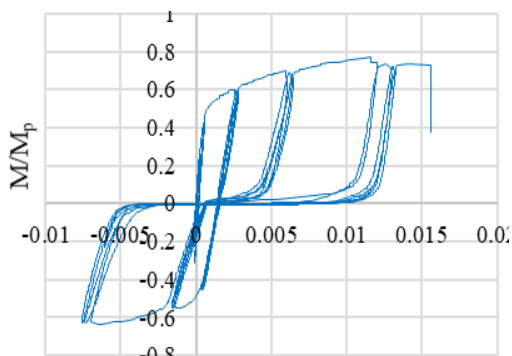


Figure 21: Hysteresis loop: moment ratio ( $M/M_p$ ) vs rotation  $\theta$

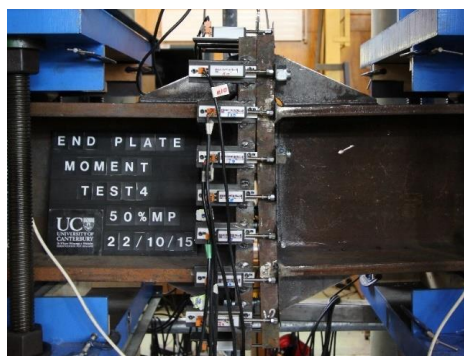


Figure 22: Deformation in Specimen #4 close to failure

## Specimen #5

This test was conducted to compare the behaviour of full penetration butt-welded splices with bolted splices. The loop shows displacement versus moment ratio at the connection. To compare the behaviour of the welded connection with bolted splice connections, the moment-displacement loop of Specimen #4 has also been presented in Figure 23.

Specimen #5 demonstrates elastoplastic performance. The test was stopped after plasticity in the smaller members due to restrictions of the test rig. No visual damage was observed in the weld after the experiment. The end plate connection performs similar to the rigid welded connection at small displacements.

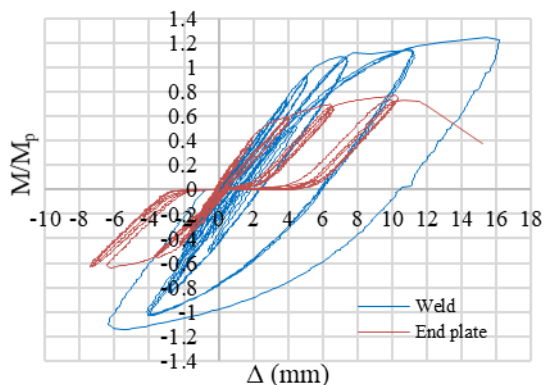


Figure 23: Hysteresis loop: moment ratio ( $M/M_p$ ) vs displacement  $\Delta$

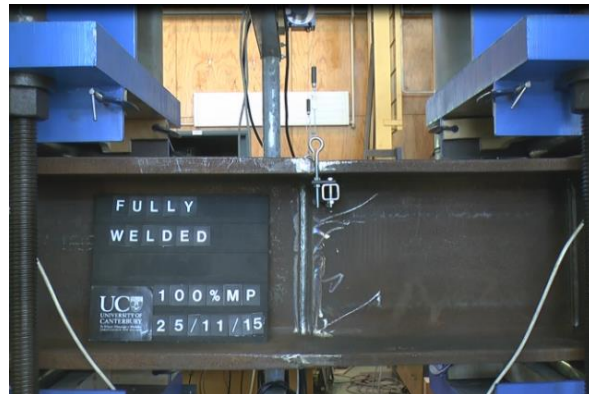


Figure 24: Specimen #8 after yielding

## 4 CONCLUSIONS

This paper describes experimental results and discussions on three types of column splice connection. It was shown that:

- In all the experiments, connections developed larger strengths than their design capacities.
- In bolted cover plate splices, the friction diminishes in larger cycles. The hysteresis loops are similar to gapping systems due to hole elongation.
- The effect of web splice plate was negligible in the overall performance of the connection due to the configuration of the connection.
- Splice connections have widely varying stiffness. The welded splice was the most rigid. The end plate splice was relatively rigid in small deformations. This connection was found to be less ductile than the lap splices, which were the most ductile.
- The stiffness and strength findings from these tests are useful for the realistic building modelling of the wide range of realistic structural configurations to determine the likely dynamic response, and develop mitigation strategies to prevent undesirable behaviour in realistic structures.

## 5 REFERENCES

- AISC. 2010. *Seismic Provisions for Steel Structural Buildings, AISC 341-10*, American Institute of Steel Construction, Chicago, IL.
- NZS3404. 1997. *Steel structures standard*. Part1. New Zealand.
- Bruneau, M. & Mahin, S.A. 1990. Ultimate Behavior of Heavy Steel Section Welded Splices and Design Implications, *Journal of Structural Engineering*, Vol 116(8) 2214–2235.

*Paper 50 – Bending stiffness and strength performance of different column splice connections*

- Stillmaker, K., Kanvinde, A. & Galasso, C. 2015. Fracture Mechanics-Based Design of Column Splices with Partial Joint Penetration Welds. *J. Struct. Eng.*
- Edwards, J.H., Whittemore, H.L. & Stang, A.H. 1929. Transverse tests of H-section column splices. *Bureau of Standards Journal of Research*, Vol 4(3) 395–413.
- Douty, R.T. & McGuire, W. 1965. High Strength Bolted Moment Connections, *Journal of structural Division*, 91.
- Beedle, L.S. & Christopher, R. 1963. Tests of steel Moment Connections, *Structural Engineers Association Proceedings*.
- Hogan, T.J. & Van der Kreek, N. 2009. *Connection Design Guide 13, RIGID CONNECTIONS*.
- Bjorhovde, R., Colson, A. & Zandonini, R. 1996. *Connection in Steel Structures III: Behaviour, Strength and Design*.
- Hogan, T.J. 2009. *Connection Design Guide 13. RIGID CONNECTIONS*.
- HERA REPORT R4-100.1. 2003. *STRUCTURAL STEELWORK CONNECTIONS GUIDE, PART1: DESIGN PROCEDURES*.